Earth Planets Space, **58**, 153–157, 2006

Large surface wave of the 2004 Sumatra-Andaman earthquake captured by the very long baseline kinematic analysis of 1-Hz GPS data

Yusaku Ohta, Irwan Meilano, Takeshi Sagiya, Fumiaki Kimata, and Kazuro Hirahara

Graduate School of Environmental Studies, Nagoya University, Nagoya 464-8602, Japan

(Received June 30, 2005; Revised December 12, 2005; Accepted December 13, 2005; Online published February 17, 2006)

The 26 December 2004 Sumatra-Andaman great earthquake had a −1500 km long rupture of more than 600 seconds duration, and may have involved a complex rupture process including slow slip. We processed International GNSS Service (IGS) 1-Hz Global Positioning System (GPS) data using kinematic analysis to investigate ground motion caused by this large earthquake. Since there are few 1-Hz stations, we had to process long baseline up to several thousand kilometers long. Long baselines degrade the GPS carrier phase ambiguity resolution. Nevertheless, clear seismic surface waves of the earthquake are recorded in our long-distance kinematic GPS solutions, which are in good agreement with response-corrected broadband seismic record. Our long baseline kinematic GPS solutions clearly indicated directivity of the seismic wave associated by rupture process of this earthquake. Also at the GPS stations that are 2,000 km away from the epicenter, dynamic displacements exceeding 5–10 cm were detected. In contrast, short baseline kinematic analysis shows large strain change caused by passage of surface wave, which reaches 6×10^{-6}. Based on the comparison with seismometer and spectrum analysis of GPS results, it is difficult to discuss for very long time period displacement such as with a period more than 600 seconds in this study.

Key words: 2004 Sumatra-Andaman earthquake, long baseline kinematic GPS analysis, broadband seismometer.

1. Introduction

The 26 December 2004 moment magnitude >9 Sumatra-Andaman earthquake generated a large Tsunami, which caused a devastating disaster including the loss of more than 180,000 lives. Ammon *et al*. (2005) described the rupture process model of this earthquake based on the seismic wave analysis including long time period seismic wave. They suggested that the northern part of the fault had a large component of slow slip, which had a 600–3500 second duration. Broadband seismometers, however, are not sensitive enough to detect these ultra-long-period slow slips.

Larson *et al*. (2003) found good agreement between strong ground-motion records integrated to displacement and 1-Hz Global Positioning System (GPS) position estimates collected more than several hundred kilometers from the 2002 Denali earthquake epicenter. They also suggested that such observations are key for studying the rupture directivity and dynamic earthquake source processes. Miyazaki *et al*. (2004) investigated rupture process of 2003 Tokachi-Oki (Hokkaido) earthquake based on high-date kinematic GPS results. They suggested that high-rate GPS is more sensitive to cumulative slip distribution. The 1-Hz GPS data enable us to have a ground displacement directly. In contrast, broadband seismometers, which measure velocity (or acceleration), must be integrated once (or twice) to get displacement data. This data processing may degrade the signal to noise ratio. Moreover, the most serious defect of broadband seismometers is the limited band compared to other seismic sensors of measurement frequency, though they have extended their frequency band. In this study, we processed GPS data using 1-Hz kinematic analysis.

2. Data and Analysis

The International GNSS Service (IGS) operated more than 200 GPS stations all over the world for the earth science research (IGS, see http://igscb.jpl.nasa.gov/). The 2004 Sumatra-Andaman earthquake began on 2004 December 26 at 00:58:53 UTC. The epicenter was located offshore the west coast of the northern Sumatra. Figure 1 shows the distribution of IGS sites around the epicenter of this earthquake. Several IGS sites record GPS data every 1 second. From these 1 second (1-Hz) GPS site, we selected 4 GPS sites; Jog Jakarta (YOGY), Bangalore (IISC), Bangalore 2 (BAN2) and Diego Garcia (DGAR) for kinematic GPS analysis (Fig. 1 and Table 1).

In this study, we used two software for the GPS data processing. For the long baseline kinematic GPS analysis, we adopted GIPSY/OASIS II (e.g. Lichten and Border, 1987). Because of a processing problem, we could not estimate kinematic positioning at BAN2 using GIPSY/OASIS II. In this background, we investigated relative deformation between BAN2 and IISC using Bernese GPS software (Hugentobler *et al*., 2001) pseudo-kinematic coordinate estimation sequence.

In the GIPSY/OASIS II, we used the Jet Propulsion Laboratory (JPL) precise orbits and clock information referred to the satellite coordinates and clock correction information. To avoid ground deformation due to seismic waves,

Table 1. Summary of kinematic GPS analysis strategy summary.

Site ID	YOGY	IISC	DGAR	MIZU	MALI	BAN2
Position (WGS-84)	110.3764°E 7.7729°S	77.5700°E 13.0210°N	72.3702°E 7.2697°S	141.1328°E 39.1352°N	40.1944°E 2.9959°S	77.5116°E 13.0343°N
Distance from epicenter (km)	2024.4	2276.3	2847.8	6055.7	6218.19	2282.6
Back Azimuth (degree)	306.46	116.74	66.69	240.76	84.07	116.71
Processing software	GIPSY-OASIS II version 2.6.0					Bernese
Elevation angle cut off	10 degrees					
Sampling interval	1 seconds					
Observation Window	00:00:00 to 01:59:59 UTC 26th December 2005					
Total Satellite in observation	12	10	12	13	12	10

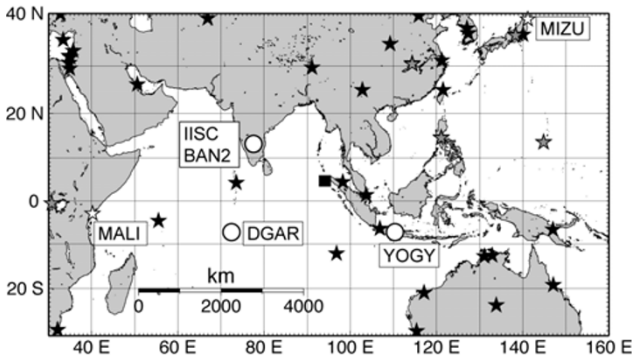

Fig. 1. Location map of epicenter of the 2004 Sumatra-Andaman earthquake and IGS GPS network. The epicenter is represented by a solid square. White stars and circles denote reference and kinematic 1 seconds sampling GPS sites, respectively. Gray and black stars denote 1 second and 30 seconds GPS stations, respectively. The stations MIZU, MALI, IISC, DGAR, YOGY and BAN2 are discussed in this study.

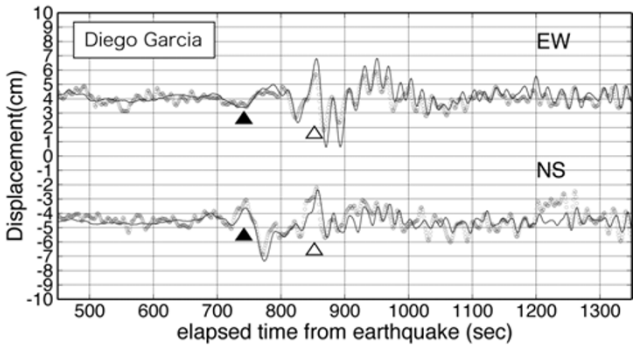

Fig. 2. Comparison of 1-Hz GPS and the response-corrected broadband seismograph record at Diego Garcia (DGAR). Small circles represent 1-Hz GPS results. Solid line denotes response-corrected seismograph record. Black and white triangles denote arrival time of Love wave and Rayleigh wave, respectively.

reference points are taken at Mizusawa (MIZU) in Japan and Malindi (MALI) in Kenya, where any no large seismic waves arrive in the time window from 00:00:00 to 01:25:00 UTC. In the GPS data analysis, receiver coordinates of kinematic GPS sites were estimated using a white noise stochastic model. The white noise has no time correlation and hence each epoch position is mutually independent. In contrast, the wet zenith tropospheric delay of all GPS sites was estimated at all observation epochs (every 1 second) under a random walk stochastic model with a random walk sigma of 1.7×10^{-7} km/sqrt (seconds). Because the baselines between the reference and Kinematic GPS sites are so long (thousands of km), GPS carrier phase ambiguities resolution was unsuccessful. We adopted so-called "bias-free" solution in this analysis. GPS satellite orbits were established and are maintained to achieve a daily repeating (sidereal period: 23 h 56 m 4 s) ground track. Multipath errors are highly repeatable from day to day (e.g. Bock, 1991). Choi *et al*. (2004) also pointed out the sidereal filter is effective for improving high-rate GPS positioning. We applied a simple sidereal filter to the kinematic GPS time series in this study.

In the Bernese GPS software, we used IGS precise orbits. The processing sequence includes (1) cycle-slip screening and outlier removal using the ionosphere free linear combination (L3) double difference phase residual, (2) ambiguity resolution using wide-lane (L5) and then L3 single difference. Since the pre-processing software of Bernese does not assume rapid changes of baseline coordinates, phase shifts caused by the displacement are erroneously recognized as cycle-slips. We summarized these GPS analysis strategies in Table 1.

Incorporated research institutions for seismology (IRIS) operates multiple seismic networks. To compare with kinematic GPS analysis, we analyzed seismic records at the DGAR (Diego Garcia) seismic station, which is located 18 km south of the GPS station. However, the difference of epicentral distances is only 2 km. At DGAR, the seismic data are recorded as velocity data by a Streckiesen STS-1 seismometer, which is broadband high gain seismometer. The velocity records were deconvolved with the instrumental response to obtain the displacements one. After deconvolution, we applied band-pass filtering to the seismometer measurements to remove long and short-term scattering. The cut-off periods of band-pass filtering are period of 10–300 seconds.

3. Results

3.1 GPS data vs. Seismometer results in Diego Garcia

Figure 2 shows a comparison of band-pass filtered (10–300 seconds) kinematic GPS analysis and response-corrected seismometer displacement at DGAR. In spite of the very long baseline kinematic analysis of more than 3,000 km, kinematic GPS results indicate remarkably a

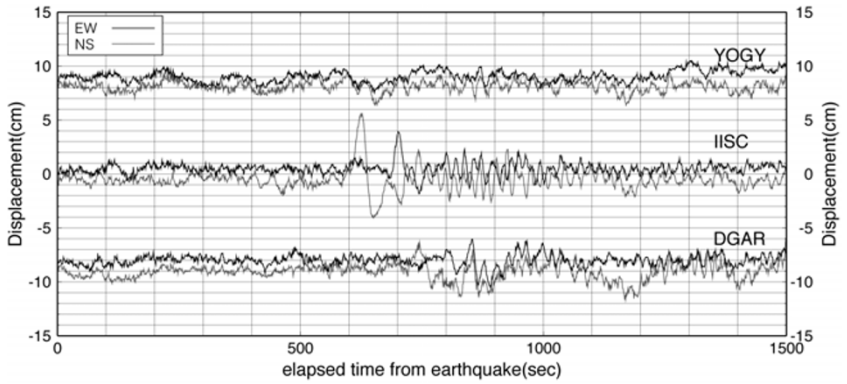

Fig. 3. Kinematic GPS observations at YOGY, IISC and DGAR. The black and gray line denotes the east-west component and north-south component, respectively. Time is seconds after the origin time of the earthquake. It is clear that IISC has characteristic large amplitude surface wave compared with another two sites.

good agreement with the response-corrected seismometer results. North-south component of the GPS time-series deviates from the seismic record around 1,000 to 1,200 seconds after the earthquake origin. The deviations are caused by the changes of satellite constellations, that is, risings and settings of GPS satellites. Due to the long distance baseline analysis, each site observes only 4–6 common GPS satellites at the same moment. The kinematic GPS results can capture completely accurately record the ground motion time history during approximately 1,000 seconds from the earthquake origin. Because DGAR is 2,847 km from the epicenter; this seismic wave should be includes the surface wave. The surface waves arrived 750 seconds after the earthquake origin. It dominants in the north-south component close to the transverse of seismic wave propagation. It has a pulse like shape with no dispersion and a group velocity with approximately 3.8 km/sec, which is interpreted to be an oceanic Love wave. Following this, the seismic waves arrived in time of 800–900 seconds in both NS and EW components are interpreted to be the Raleigh waves with normal dispersion (Fig. 2).

3.2 Another GPS sites

Figure 3 shows time series of kinematic analysis at three GPS sites. It is clear that north-south component at IISC shows a large oceanic Love wave in the time of 600 to 700 seconds after the earthquake, whose with a maximum amplitude reaches of approximately 9 cm. The station IISC is located northwestward from the epicenter at 2,276 km. Although YOGY is similarly located in 2,026 km from the epicenter, the seismic signal is very small compared with IISC. DGAR also small compared with IISC. In spite of the almost similar distance from the epicenter, the displacements time at YOGY have less than 4 cm amplitude. These differences clearly indicate the directivity of rupture process in this earthquake (e.g. Lay *et al.*, 2005). Figure 4(a) shows the time series of short baseline GPS analysis between BAN2 and IISC using Bernese GPS software. The maximum peak to peak displacement reaches 4 cm with a period of 7–8 seconds.

4. Discussion

In this study, we executed GPS kinematic solution for very long baselines and short baseline using GIPSY/OASIS

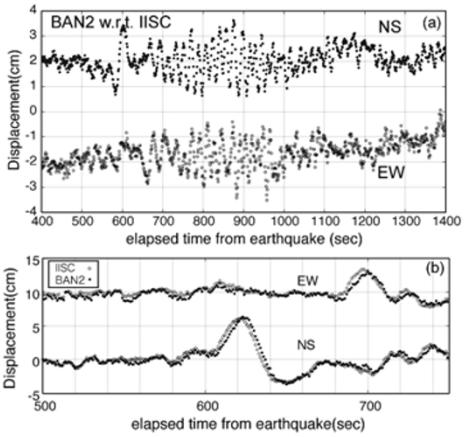

Fig. 4. (a) Displacements at station BAN2 relative to IISC. Time is seconds after the origin time of the earthquake. Black and white circles denotes north-south and east-west component, respectively. (b) Comparison of absolute component displacement at IISC and synthesized displacements at BAN2. White circles denote observed displacement time series at IISC. Black circles show synthesized time series at BAN2.

II and Bernese GPS software, respectively. As the reference sites do not suffer from deformation due to the seismic waves during 25 minutes from the earthquake origin, the long baseline solutions indicate absolute displacements. In contrast, the short baseline results show relative displacement, because the reference sites also involve displacement for the arrival of a seismic wave. In this section, we explain abilities of the short and long baseline kinematic GPS analysis, respectively.

4.1 Large strain change observed by short baseline analysis

Because of processing problem, we failed to determine the displacements at BAN2 from the far reference sites. Therefore, we tried to synthesize the absolute displacement of BAN2 from the very long baseline solution at IISC and relative short baseline solution at BAN2 from IISC (Fig. 4(a)). Figure 4(b) shows a comparison of the observed absolute displacement in the north-south and east-west components at IISC and the synthesized on at BAN2. The seismic waves were observed at 610 seconds after the earthquake origin, and it shows clear phase lag of about 1

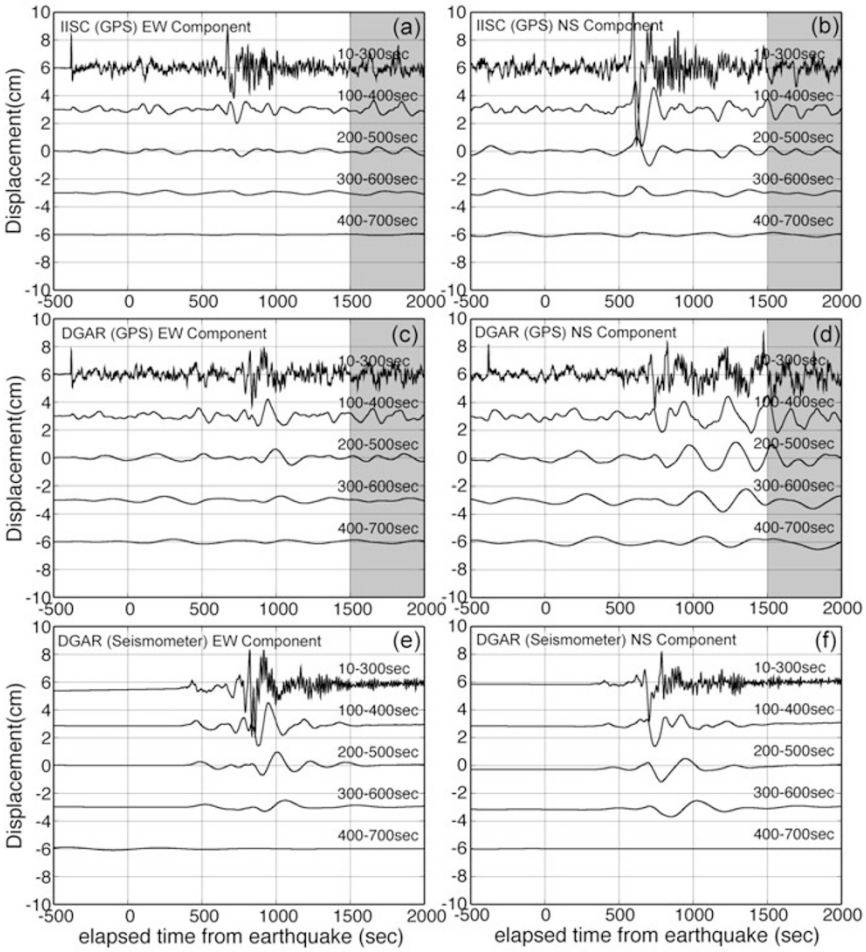

Fig. 5. Band-pass filtered time series of GPS and seismometer results. Each panel contains a different band-pass filtered on 10–300, 100–400, 200–500, 300–600 and 400–700, respectively. Time is seconds after the origin time of the earthquake. Shadowed part denoted arriving the seismic wave to reference site of GPS.

to 2 seconds between the arrival times at IISC and BAN2. The epicentral distance at IISC is 6.4 km shorter than BAN2. The phase lag of 1–2 seconds is consistent with the oceanic Love wave group velocity of 3.7–3.8 km/sec. This passage of the surface wave indicates large dynamic strains. In spite of the only 7 km baseline length, passage of the surface wave generated maximum up to 4 cm amplitude peak-to-peak relative displacement between BAN2 and IISC (Fig. 4(a)); the strain reaches 6×10^{-6} between two sites. West *et al*. (2005) indicated that Rayleigh waves from this earthquake triggered an earthquake swarm near Mount Wrangell in Alaska based on seismometer observations. In our study, however, there is no information that seismic activities change around BAN2 and IISC.

4.2 Sensitivity of long baseline kinematic GPS analysis

Ammon *et al*. (2005) suggested that northern part of the fault had large slow slip, which had duration of 600-3500 seconds duration time. Figure 5 show that band-passed filtering time series results of kinematic GPS and integrated seismometer results in different cut-off periods, which are 10–300, 100–400, 200–500, 300–600 and 400–700 seconds. The seismometer results (Fig. 5(e) and (f)) shows up to around 400 seconds time periods surface wave. However, there is no significant long time period displacement such as over 400 seconds. It is consistent with band-limit of STS-1 broadband seismometer (up to 360 seconds). The kinematic GPS results (Fig. 5(a), (b), (c) and (d)) also detected surface wave with around 400 seconds time periods. We omit after 1,500 seconds for discussion to avoid ground shaking for arrival of seismic wave to reference sites (denoted by shadowed). The north-south component of DGAR (Fig. 5(d)) is extremely noisy around the 1,300 seconds. It is mainly caused by bad satellites constellation effect. Along with the seismometer results, kinematic GPS analyses show no significant long time period displacement. These results suggest two possibilities. 1) There is no long time period displacement in this earthquake. 2) It is not enough sensitivity to detect for long time period displacement such as more than 600 seconds in our analysis.

For classification, we discuss in the frequency domain representations of a kinematic GPS time series. Mao *et al*. (1999) investigated that the noise characteristic in daily position of GPS data. They concluded a combination of white noise and flicker noise appears to be the best model for the noise characteristics. Bock *et al*. (2000) suggested GPS single-epoch solutions indicates that the flicker noise characteristic in the frequency band 0.01 mHz to 10 mHz. Therefore, we can expect almost flicker noise characteris-

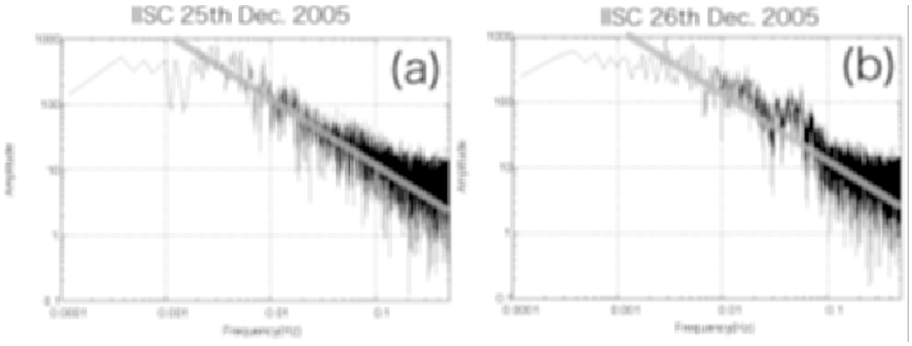

Fig. 6. Fourier spectrum amplitude showed in the IISC IGS station 1-Hz kinematic GPS time series. (a) Time period was 25th December 2005 during 00:00:00–02:00:00 (GMT). White line denoted 1/frequenct gradient. (b) Time period was 26th December 2005 during same time period as Fig. 6(a).

tic for our power-spectrum of kinematic GPS time series. Figure 6(a) and (b) show the power spectrum of 2 hours kinematic GPS time series in for IISC on 25th and 26th December 2004, respectively. There is no large seismic event in 25th December 2004. Therefore, Fig. 6(a) shows the noise level in our GPS kinematic solution. The noise-level is increasing linearly with 1/f gradient (denoted white dashed line) between 0.1 Hz and 0.0025 Hz (10–400 seconds) (Fig. 6(a)). It shows that in the period of 0.1–0.0025 Hz, which indicate enough sensitivity in our GPS kinematic solution. In contrast, the 26th December record shows noise plus seismic signal, which shows power above the noise level from about 0.03 to 0.08 Hz and down to perhaps 0.002 Hz (Fig. 6(b)). Presumably the noise spectrum is similar on the two days, but the seismic signal is the difference. Unfortunately, our results look like for the frequencies needed to investigate for long time period displacement such as more than 600 seconds. It is not depend on the sampling interval. It is caused by noise-related problem associated with temporal variations in multipath, atmospheric delay or other systematic error source inherent to kinematic GPS analysis.

According to these discussions, it is difficult to discuss for existence of long time period displacement (e.g. over 600 seconds) in this study. Our kinematic GPS analysis sensitivity is slightly not enough to detect very long time period displacement. Though, our GPS result provides comparable sensitivity to broadband seismometer such as STS-1. If we can improve the noise-related problem of GPS associated with temporal variation, we can possible to expect better sensitivity in long time period.

5. Conclusions

In this study, we perform short and very long baseline kinematic GPS analysis. Our long baseline results show clear directivity of the seismic wave along toward the north-west direction. In contrast, a short baseline result indicates large strain change associated by passage of the surface wave. Our long baseline solution indicates that sensitivity of 2-hours kinematic GPS time series is slightly not enough to discuss very long time period seismic wave. However, our kinematic GPS results show comparable sensitivity with broadband seismometer.

Acknowledgments. Comments from Prof. Yuichiro Tanioka, Prof. Jeff Freymueller, and one anonymous reviewer significantly improved the manuscript. We are grateful thanks to Dr. Shin'ichi Miyazaki (ERI, Tokyo University) for advices of GPS processing. We are grateful to International GNSS Service (IGS) for providing GPS data. We also appreciate incorporated research institutions for seismology (IRIS) data center for providing seismic record data.

References

Ammon, C. J., C. Ji, H.-K. Thio, D. Robinson, S. Ni, V. Hjorleifsdottir, H. Kanamori, T. Lay, S. Das, D. Helmberger, G. Ichinose, J. Polet, and D. Wald, Rupture process of the 2004 Sumatra-Andaman earthquake, *Science*, 20 May, 1133–1139, 2005.

Bock, Y., Continuous monitoring of crustal deformation, *GPS World*, **2**(6), 40–47, 1991.

Bock, Y., R. M. Nikolaidis, P. J. de Jonge, and M. Bevis, Instantaneous geodetic positioning at medium distances with the Global Positioning System, *J. Geophys. Res.*, **105**(B12), 28,223, (2000JB900268), 2000.

Choi, K., A. Bilich, K. Larson, and P. Axelarad, Modified Sidereal filtering: Implications for high-rate GPS positioning, *Geophys. Res. Lett.*, **31**, L22608, 2004.

Hugentobler, U., S. Schafer, and P. Fridez, Bernese GPS software Version 4.2., Astronomical Institute University of Berne, 515 pp., 2001.

Larson, K., P. Bodin, and J. Gomberg, Using 1-Hz GPS data to measure deformations caused by the denali fault earthquake, *Science*, **300**, 30 May, 2003.

Lay, T., H. Kanamori, C. J. Ammon, M. Nettles, S. N. Ward, R. C. Aster, S. L. Beck, S. L. Bilek, M. R. Brudzinski, R. Butler, H. R. DeShon, G. Ekström, K. Satake, and S. Sipkin, The Great Sumatra-Andaman Earthquake of 26 December 2004, *Science*, 20 May, 1127–1133, 2005.

Lichten, S. M. and J. S. Border, Strategies for high precision global positioning system orbit determination, *J. Geophys. Res.*, **92**(B12), 12751–12762 Nov 10, 1987.

Mao, A., C. G. A. Harrison, and T. H. Dixon, Noise in GPS coordinate time series, *J. Geophys. Res.*, **104**(B2), 2797 (1998JB900033), 1999.

Miyazaki, S., K. M. Larson, K. Choi, K. Hikima, K. Koketsu, P. Bodin, J. Haase, G. Emore, and A. Yamagiwa, Modeling the rupture process of the 2003 September 25 Tokachi-Oki (Hokkaido) earthquake using 1-Hz GPS data, *Geophys. Res. Lett.*, **31**, L21603, doi:10.1029/2004GL021457, 2004.

West, M., J. J. Sanchez, and S. R. McNutt, Periodically Triggered Seismicity at Mount Wrangell, Alaska, After the Sumatra Earthquake, *Science*, 20 May 2005, 1144–1146, 2005.

Y. Ohta (e-mail: oota@eps.nagoya-u.ac.jp), I. Meilano (e-mail: irwan@eps.nagoya-u.ac.jp), T. Sagiya (e-mail: sagiya@seis.nagoya-u.ac.jp), F. Kimata (e-mail: kimata@seis.nagoya-u.ac.jp), and K. Hirahara (e-mail: hirahara@eps.nagoya-u.ac.jp)